Fatigue and Fracture of Bovine Dentin

by D. Arola, J. A. Rouland and D. Zhang

ABSTRACT—In this paper, the fatigue and fracture properties of bovine dentin are evaluated using *in vitro* experimental analyses. Double cantilever beam (DCB) specimens were prepared from bovine maxillary molars and subjected to zero-to-tension cyclic loads. The fatigue crack growth rate was evaluated as a function of the dentin tubule orientation using the Paris law. Wedge-loaded DCB specimens were also prepared and subjected to monotonic opening loads. Moiré interferometry was used to acquire the in-plane displacement field during stable crack growth, and the instantaneous wedge load and crack length were acquired to evaluate the crack growth resistance and crack tip opening displacement (CTOD) with crack extension. The rate of fatigue crack growth was generally larger for crack propagation occurring perpendicular to the dentin tubules. The Moiré fringe fields documented during monotonic crack growth exhibited non-linear deformation occurring within a confined region adjacent to the crack tip. Both the wedge load and CTOD response provided evidence that a fracture process zone contributes to energy dissipation during crack extension and that dentin exhibits a rising R-curve behavior. Results from this preliminary investigation are being used as a guide for an evaluation of the fatigue and fracture properties of human dentin.

KEY WORDS—Dentin, fatigue, fracture process zone, Moiré interferometry, teeth

Introduction

Restorative dentistry plays an important role in the maintenance of oral health. A restoration generally involves removing tissue that has been destroyed or undermined from bacterial invasion, preparing a suitable cavity, and filling this reservoir with a structural material of adequate strength and stiffness. Assuming that all bacteria are removed and no other insults are caused by the cavity preparation, oral function of the tooth is "restored." Nevertheless, the probability of restored tooth failure can exceed 40 percent.[1]

Though not the primary mode of restored tooth failure, tooth fracture may be the most detrimental as it often results in sub-gingival terminations that require extraction.[2] According to independent clinical surveys, over 90 percent of fractured teeth have been previously restored.[2,3] The problem is so prominent that it has been coined the "cracked tooth syndrome" (see, for example, Ref. 4). In response to this problem an examination of first and second molars with mesial occlusal distal (MOD) amalgam restorations has recently been conducted. These teeth were extracted from patients at the University of Maryland Dental School for reasons other than tooth fracture. The molars were sectioned and examined using an optical microscope. In an inspection of the internal line angles or regions adjacent to the interface of the tooth and restoration, it was found that cracks were present in nearly half of the molars examined (Fig. 1). These observations suggest that mechanical failure of restored teeth is facilitated by fatigue crack growth and that tooth fracture occurs when the crack propagates to a critical length. With patients retaining their teeth for a longer period of their life, tooth cracking and restored tooth fracture could become a significant obstacle to lifelong oral health. Therefore, a better understanding of the fatigue and fracture properties of the tooth is clearly needed.

Background

The tooth proper is comprised of three unique tissues including the enamel, dentin and pulp. Dentin comprises the majority of the tooth by volume (Fig. 2) and serves as an elastic foundation for the enamel and as a protective enclosure for the pulp. Considered a hard tissue, the dentin is approximately 50 percent inorganic, 30 percent organic, and 20 percent fluid.[5] Dentin is traversed by tubules that extend from the pulp towards the dentin-enamel junction (DEJ). Both their size and density decrease with distance from the pulp. Typical tubule diameters in coronal dentin have been reported to be 2.5 μm near the pulp and reduce to 0.8 μm at the DEJ.[6] The tubule boundaries are lined by peritubular dentin, a highly mineralized cuff that consists of apatite crystals with negligible organic content.[5] Intertubular dentin is of higher organic content due to the presence of an apatite reinforcing collagen fibril network. These structural components have been found to be important to the mechanical properties of dentin.[7,8] A complete review of the structure and mechanical properties of dentin is available in Ref. 9.

Due to the importance of tooth fracture to the survival of restored teeth, the fracture toughness (K_{Ic}) of dentin and enamel has been estimated using various methods.[10–14] According to these studies the average K_{Ic} of human dentin is 3.0 Mpa $m^{0.5}$. Iwamoto and Ruse[15] recently reported that the fracture toughness of dentin was anisotropic; the K_{Ic} determined for crack propagation perpendicular to the tubules was significantly lower than that for growth parallel to the tubules. Similarly, the K_{Ic} of enamel is reportedly anisotropic and is 0.7 and 1.5 Mpa $m^{0.5}$, respectively, in directions parallel and perpendicular to the enamel prism.[14] Based on the

D. Arola is an Assistant Professor, J.A. Rouland is a Ph.D. student, and D. Zhang is currently an Associate Research Scientist, Department of Mechanical Engineering, University of Maryland Baltimore County, 1000 Hilltop Circle, Baltimore, MD 21250. D. Zhang is also an Associate Professor, Department of Astronautical Technology, National University of Defense Technology, Changsha 410073, People's Republic of China.

Original manuscript submitted: February 26, 2002.
Final manuscript received: August 7, 2002.

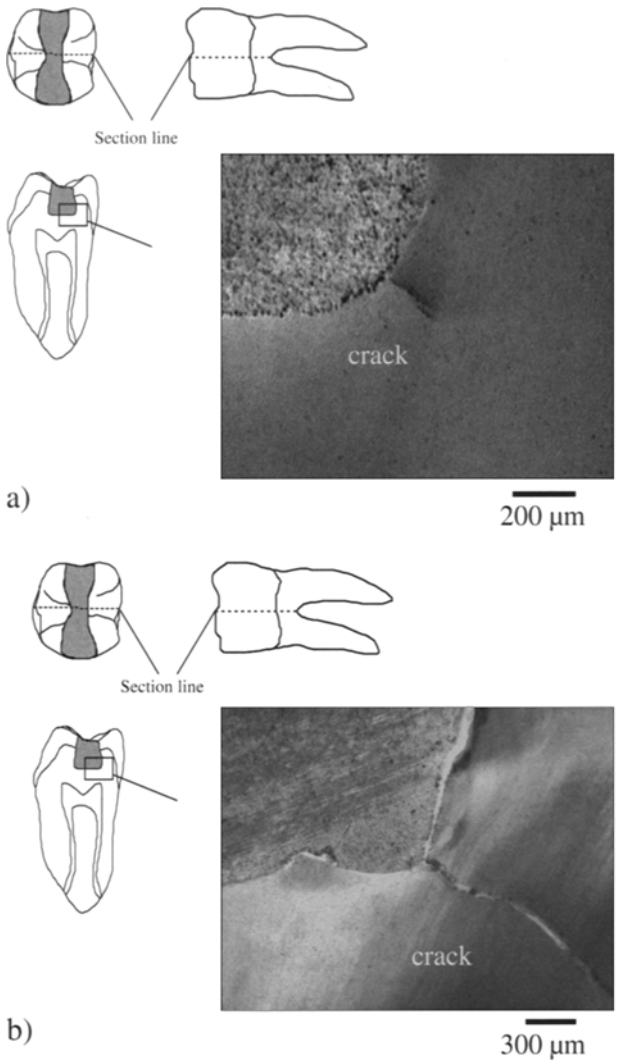

Fig. 1—Cracks evident along the internal line angles of two different restored molars. The crack orientation is perpendicular to the dentin tubule orientation in both molars

quasi-brittle nature and anisotropic biological structure of both tissues, the mechanisms of crack growth and energy dissipation in dentin and enamel are not obvious. Furthermore, noted changes in strength and elastic modulus of dentin with demineralization[16,17] suggest that the mechanisms of energy dissipation may also change with aging or other biological processes. However, no study has reported on the mechanics of fracture and the mechanisms of energy dissipation associated with crack growth in dentin or enamel.

Due to the prevalence of tooth cracking in restored teeth, an investigation of the fatigue and fracture properties of dentin is warranted. But an investigation of this type is notably restricted by the size of human teeth. Bovine molars are much larger than human teeth and permit an analysis of mechanical properties with only minimal restrictions posed by the specimen size. In addition, recent studies have reported that the structure of human and bovine dentin is very similar.[18,19] Therefore, in this preliminary investigation the fatigue and fracture properties of bovine dentin have been evaluated as a model for human dentin. The study is ongoing and these preliminary results are being used in refining the

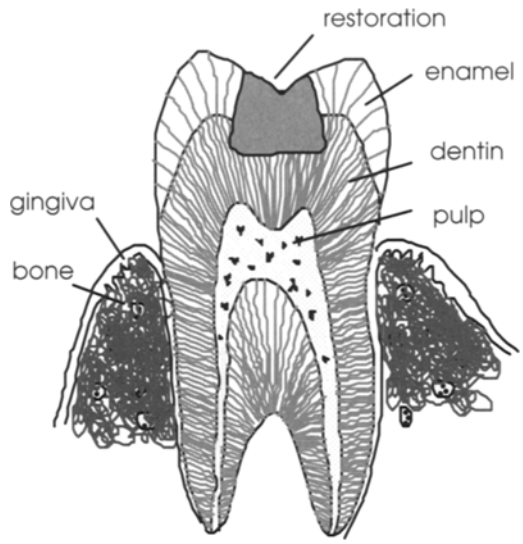

Fig. 2—Schematic cross section of a restored molar highlighting the primary tissues

experimental methods for an investigation of the fatigue and fracture properties of human dentin.

Materials and Methods

Fresh non-carious maxillary molars were extracted from mature bovine (between one and three years of age) within approximately twelve hours of sacrifice. The teeth were cast within a cylindrical ring fixture using a polymeric resin and then sectioned with diamond impregnated abrasive wheels using a numerically controlled grinder/slicer (K.O. Lee slicer/grinder, Model 3818 HSS, Aberdeen, SD). All specimen preparation was conducted under continuous flood coolant to maintain the tissue hydration. Primary sectioning was conducted along the mesial/distal axis of the crown (Fig. 3(a)) with a commercial diamond impregnated slicing wheel with 220 mesh abrasives. Secondary sections were introduced as required for the desired specimen geometry and dentin tubule orientation.

Double cantilever beam (DCB) specimens and wedge-loaded DCB (WL-DCB) specimens were machined from mesial distal sections of the extracted molars. The DCB specimens (Fig. 3(b)) were used for the cyclic crack growth experiments whereas the WL-DCB specimens (Fig. 3(c)) were used to evaluate stable crack growth resulting from monotonic loads. A longitudinal groove of 0.30 mm width was introduced in both specimen types using a 320 mesh diamond abrasive slicing wheel; the groove channels the direction of crack growth during cyclic or monotonic loading. Holes were drilled in the DCB specimens using a miniature CNC milling machine (Dyna Myte CNC Milling Machine, Model 2400, El Segundo, CA) to enable the application of cyclic loads. The notch tip of each specimen was sharpened using a razor blade and 6 μm diamond paste, which serves to facilitate stable crack initiation for both monotonic and cyclic loading.

Fatigue Crack Growth

The dentin DCB specimens were subjected to zero-to-maximum opening (mode I) loads with an EnduraTEC ELF

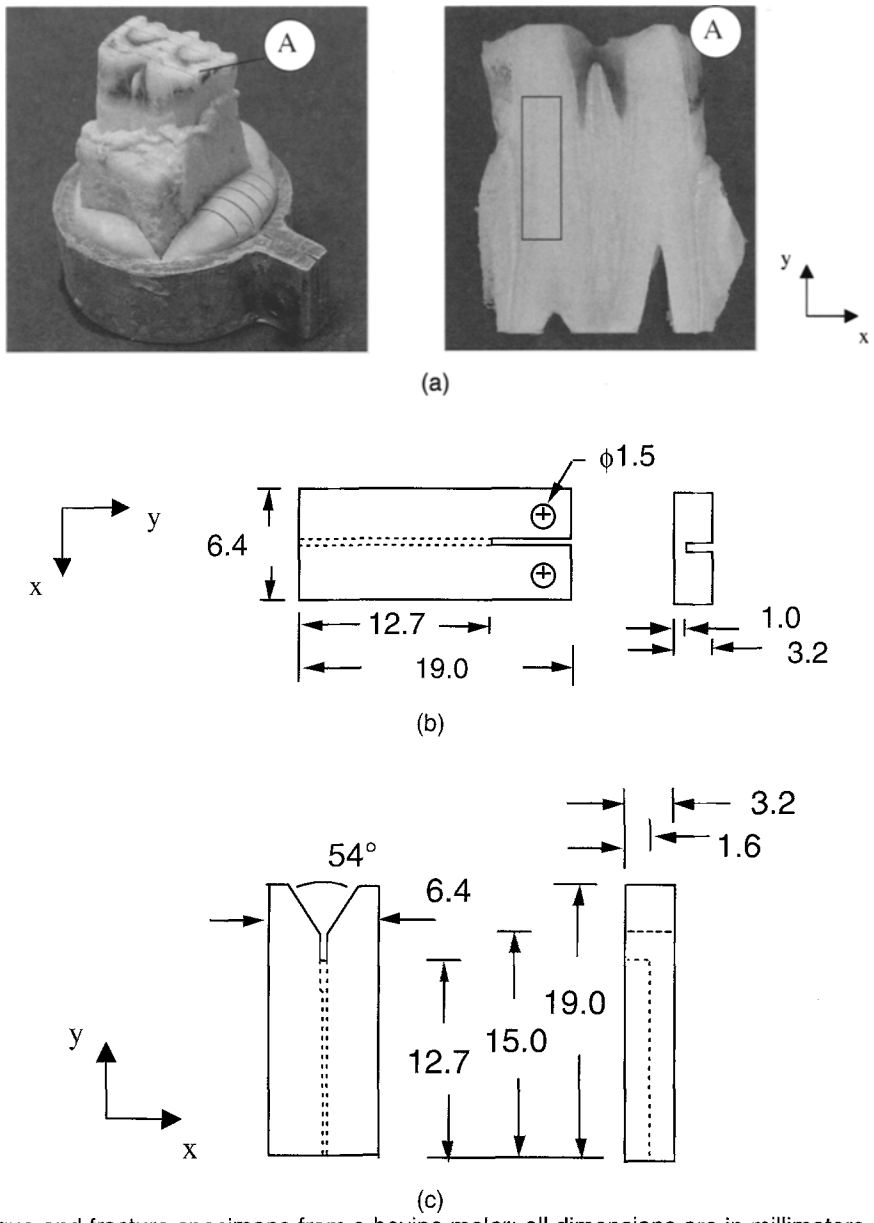

Fig. 3—Obtaining fatigue and fracture specimens from a bovine molar; all dimensions are in millimeters. Tubule orientation is defined with respect to the y-axis (i.e., the tubules for 0° dentin are oriented parallel to the y-axis). (a) A sectioned bovine molar mounted in a polymer resin and an outline of a potential specimen from a single mesial-distal section; (b) DCB specimen; (c) WL-DCB specimen

Model 3200. The system has a maximum load capacity of 225 N and sensitivity of ±0.01 N. Special grips were fabricated to enable the application of fatigue loads through stainless-steel pins that extend through the drilled holes. The specimens were subjected to load-control fatigue using a maximum tensile load (P) of between 10 and 16 N, and a frequency between 2 and 5 Hz. The frequency and magnitude of fatigue loading are chosen according to the rate of crack growth observed during crack initiation and the desired time interval between successive crack length measurements. A calcium and phosphate containing buffered saline medium (21°C) was used to maintain the specimen's moisture content during fatigue loading.

The ungrooved surface of the DCB specimens was accentuated with dilute (approximately 5 percent) silver nitrate to heighten contrast between the crack and dentin. After specific intervals of fatigue loading, the saline bath was drained and the crack length was measured visually using a scaled optical microscope (60×). The fatigue increment between measurements (ΔN) was chosen according to the observed growth rate and ranges between every 25,000 to every 100,000 cycles. The fatigue crack growth rate $\left(\frac{da}{dN}\right)$ was evaluated using the crack length measurements in terms of the Paris law[20] according to

$$\left.\frac{da}{dN}\right|_{\theta} = C(\Delta K)^m, \qquad (1)$$

where C and m are the fatigue crack growth coefficient and exponent, respectively, da is the increment of crack extension and ΔK is the stress intensity range. The growth rate

was evaluated as a function of tubule orientation (θ) to identify differences in crack propagation related to the tissue's structure. Three primary tubule orientations have been chosen for the preliminary study including 0°, 45°, and 90°, with respect to the crack surface; the preliminary results reported here are limited to results for the 0° and 90° orientations. Fatigue crack growth within each specimen was monitored from crack initiation to fracture. An experiment typically spanned a period of two to four days, and depended on the extent of stable crack growth achieved and the incidence of crack curving. Following fracture, the specimens were sputtered with gold palladium and the fracture surface morphology was examined using a JEOL JSM-5600 scanning electron microscope (SEM).

Monotonic Crack Growth

Stable crack growth in the dentin specimens was monitored using Moiré interferometry and required the application of a suitable grating. The standard technique generally used to transfer the grating is not appropriate for the dentin specimens since the moisture content must be preserved during the experiments. Therefore, a new approach was adopted which incorporates a simple modification of the standard replication process.[21] Initially, the ungrooved surface of the WL-DCB dentin specimens was polished using aluminum oxide 600 mesh abrasive paper. Also, the sub-master mold photoplate was liberally coated with dilute photo flow to assist in uniform mold release. Based on the elastic modulus of dentin[16] and expected magnitude of displacement during wedge loading, a grating with frequency of 600 lines mm^{-1} was selected for application. After allowing the photoplate to dry, it was sputtered with a 200 nm layer of highly reflective aluminum at a rate of approximately 0.4 nanometers per second. A thin layer of epoxy (PC-10, Measurements Group, Raleigh, NC) was then applied to the sputtered photoplate surface and placed on a flat glass plate covered with Teflon (for release). The epoxy film was allowed to dry for 24 h after which the sub-master mold and glass plate were carefully separated. Using this process, a hardened layer of epoxy, approximately 25 μm thick, formed on the back side of the grating. The hydrated bovine WL-DCB specimens were then glued to the epoxy layer with cyanacrolate (superglue) along the ungrooved surface. The epoxy film is much less permeable than the sputtered aluminum coating, and serves as a cohesive medium for bonding of the cyanacrolate. Within 5 min of bonding, the mold was removed and the specimen was ready for testing.

The WL-DCB fracture specimens were placed within a rigid fixture for displacement controlled wedge loading. Only the u-field specimen displacement (in the x-direction) was recorded which is perpendicular to the direction of crack extension and reflects the opening displacement. The nature of loading and change in compliance with crack propagation results in v-field displacement that is negligible in comparison; the v-field was not recorded in this preliminary study. The optical system utilized in this investigation consisted of a 10 mW He-Ne laser, a spatial filter, a collimating lens, a two-beam interferometer, appropriate supplementary mirrors, and a 35 mm camera (Fig. 4). Interference of the two oblique beams generated a reference grating in front of the specimen of 1200 lines mm^{-1}. Upon application of wedge loads, deformation in the specimen caused distorted diffraction of

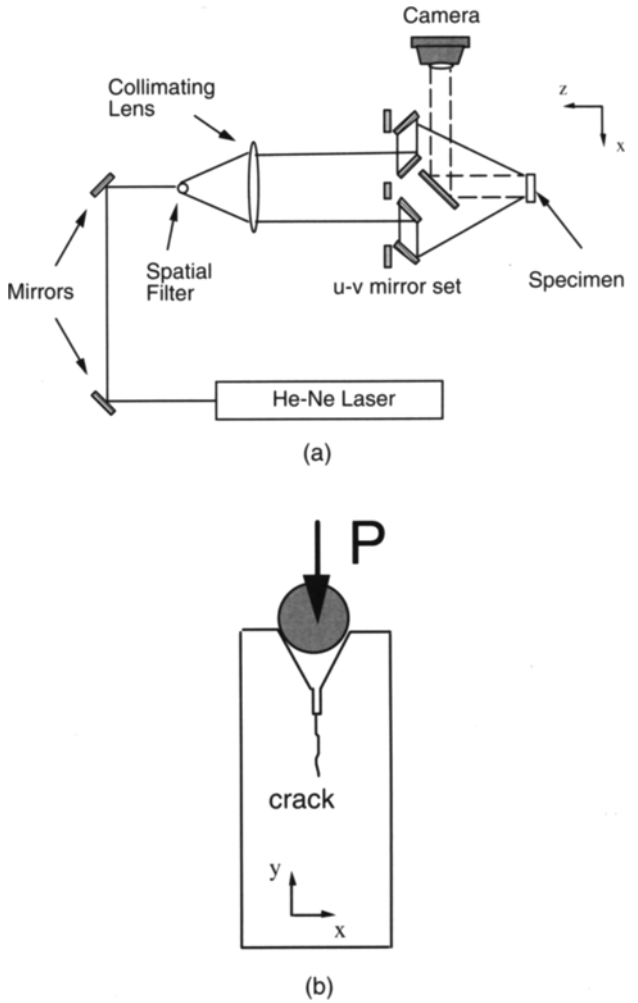

Fig. 4—Schematic diagrams of the optical arrangement and wedge loading process utilized for examining stable crack growth: (a) optical arrangement; (b) wedge loading

the orders of ± 1 to interfere with the undistorted reference grating, and resulted in an interference Moiré fringe pattern in front of the specimen. Moiré fringe patterns were then reflected by a mirror to the 35 mm camera for documentation.

Monotonic loads were applied to the WL-DCB specimens in increments of 2.3 N through a stainless-steel pin of 4.76 mm diameter (Fig. 4). Moiré fringes were recorded at the peak load of each increment of pin displacement. The crack length, unit of crack extension, and pin displacement were not recorded during the loading process because the crack position at each load increment was available (and more accurately obtained) from the Moiré fringe field. The incremental wedge loading for each specimen was continued until the crack resulted in catastrophic fracture of the specimen or discontinued after a sufficient extent of growth. On average, each test lasted approximately 30 min and was dependent on the extent of stable crack growth achieved. Hydration of the specimens was maintained during wedge loading by applying tap water through an eyedropper along the back side opposite to the surface facing the interferometer. The Moiré fringe pattern recorded at each load increment was digitized and then examined using commercial software (Adobe Illustrator, Version 8.0, San Jose, CA). For each load increment of extension the number of fringes was counted from the zero

fringe to the point of interest. The fringe number (N) was converted to the corresponding magnitude of displacement (u) according to[21]

$$u(x, y) = \frac{1}{f} N(x, y), \tag{2}$$

where f is the reference grating frequency (lines mm^{-1}). Due to the symmetry of the WL-DCB specimens, the zero fringe order, representing the point of zero opening displacement, is located at the crack tip. Both the magnitude of the opening mode displacement at the pin contact, and the crack opening displacement behind the crack tip, were estimated at each load increment according to eq (2). The crack tip opening displacement (CTOD) was estimated over the extension history from the opening displacement at a distance 1 mm behind the crack tip.

Results

Fatigue crack growth rates resulting from cyclic mode I loading of the DCB bovine dentin specimens are shown in terms of the stress intensity range in Fig. 5. Assuming a power-law response according to eq (1), the crack growth exponent and coefficient were determined from the slope and y-intercept of the cyclic response of each specimen; these are listed in Table 1. From a comparison of the growth responses in Fig. 5, it is evident that the lowest growth rate occurred in specimens that had dentin tubules oriented parallel (0°) to the direction of crack propagation. The average crack growth exponent (m) estimated for propagation perpendicular (90°) to the tubules was 4.24, slightly lower than that for crack growth parallel to the dentin tubules (4.36). In general, a large variation in the fatigue crack growth rate was evident from the results of the three specimens with each of the two dentin tubule orientations. Fatigue crack growth was also evaluated using the WL-DCB specimen configuration and proceeded more rapidly than in the standard DCB dentin specimens; the crack growth exponent was found to be 6.78. Stable crack growth was difficult to maintain in the WL-DCB dentin specimens and all future evaluations will be conducted with the standard DCB specimen.

Typical SEM micrographs of the fracture surfaces from dentin specimens are shown in Fig. 6 and differences related to the tubule orientation are clearly apparent. Dentinal tubules are evident and are highlighted in each of these figures. The fracture surface morphology for crack growth parallel to the tubule orientation (Fig. 6(a)) is smooth and much more uniform than that for crack growth perpendicular to the tubules (Fig. 6(b)). The surface of specimens resulting from crack growth perpendicular to the tubules reveals an irregular and notably rough surface (Fig. 6(b)) with a texture very different from that in which fracture occurred parallel to the tubule axis (Fig. 6(b)). Crack propagation occurring perpendicular to the tubules appeared to plastically deform the dentinal matrix. Interestingly, peritubular cuffs were found extending from the fracture surfaces or pulled out of the intertubular matrix of specimens that underwent crack growth perpendicular to the tubules. In contrast, the fracture surface of specimens with 0° tubule orientation did not exhibit any unique elements extending from the fracture surface. Based on the SEM analysis, crack growth parallel to the tubules appeared to have proceeded in a more brittle manner.

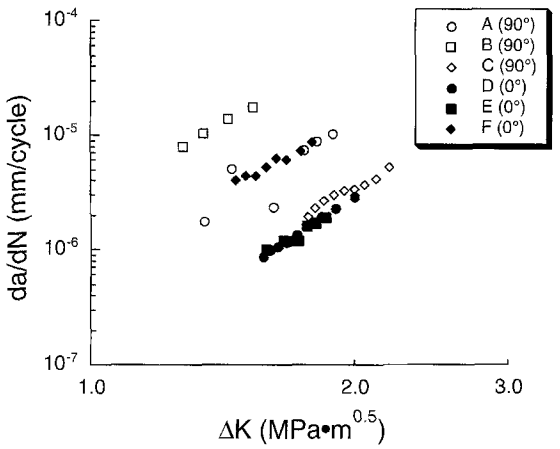

Fig. 5—Preliminary results of the fatigue crack growth experiments. The growth rates presented in this figure result from mode I loading of the DCB bovine dentin specimens. The Paris law parameters for each of these specimens are listed in Table 1

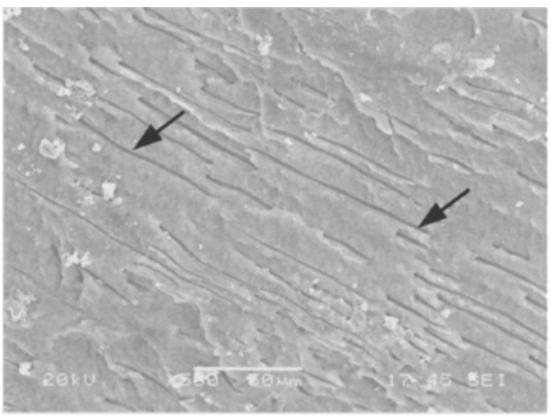

(a)

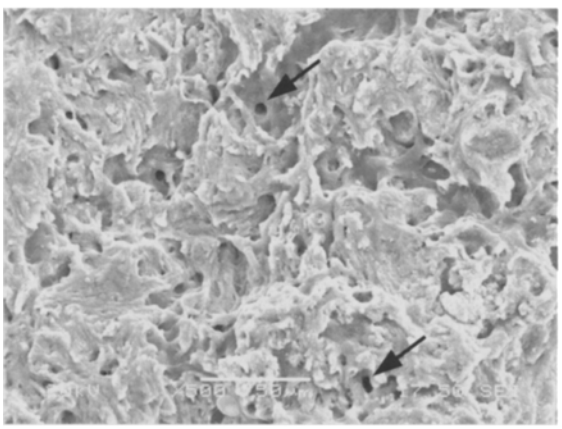

(b)

Fig. 6—SEM micrographs of the fracture surface from the dentin DCB specimens. Distinct tubules are highlighted in each micrograph by the arrows. (a) Fatigue crack growth parallel to the dentin tubules (x500); (b) fatigue crack growth perpendicular to the dentin tubules (x500)

TABLE 1—FATIGUE CRACK GROWTH PARAMETERS FOR BOVINE DENTIN

Specimen	Orientation* (°)	C (mm cycle^{-1})(Mpa m$^{0.5}$)$^{-m}$	m
WL-DCB	N/A	8.00×10^{-10}	6.78
DCB			
A	90	5.48×10^{-7}	4.48
B	90	2.87×10^{-6}	4.28
C	90	2.19×10^{-7}	3.97
D	0	9.03×10^{-8}	5.02
E	0	1.33×10^{-7}	4.27
F	0	9.11×10^{-7}	3.78

*The dentin tubule orientation relative to the plane of crack growth

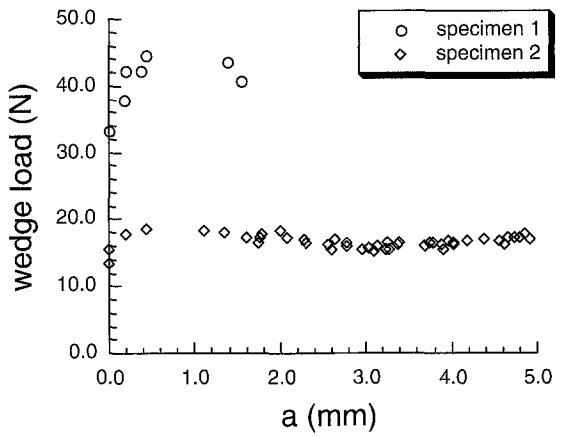

Fig. 7—Wedge load history during stable crack growth in the dentin WL-DCB specimens

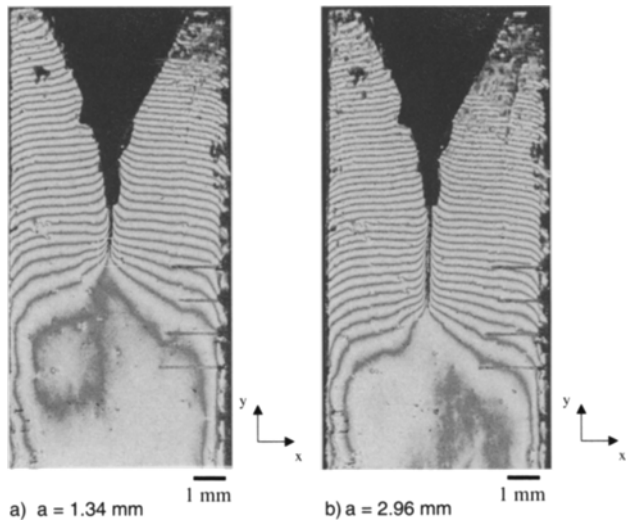

Fig. 8—Moiré fringe patterns (u-field) resulting from wedge loading of a WL-DCB dentin specimen at different increments of crack growth: (a) a = 1.34 mm; (b) a = 2.96 mm. The highlighted region in (a) is shown in Fig. 9

Figure 7 shows the wedge-load distribution with crack extension that was recorded during stable crack growth within two bovine dentin specimens; the dentin tubule orientation of these specimens with relation to the direction of crack growth was not identified. Each of these specimens was obtained from a different cow. As evident from a comparison of the load profiles in Fig. 7, notable differences in the fracture behavior were observed. Specimen 1 required more than twice the wedge load to initiate crack growth but became unstable after only 1.5 mm of extension. The second specimen required much lower driving force for extension but achieved 5 mm of stable crack growth. Despite these differences, both specimens exhibited an initial rise in load with crack extension suggesting that dentin exhibits a rising fracture toughness (rising R-curve) with crack extension. The load response for both bovine dentin specimens reached steady state, or the maximum value, at approximately 0.5 mm of crack growth.

Using the load and crack length measurements determined from the crack extension profiles in Fig. 7, the energy release rate (G) was estimated according to beam theory and Irwin's energy model.[22] The fracture toughness (K) was calculated from knowledge of G and the elastic modulus of bovine dentin. Though generally calculated at crack initiation, both G and K were calculated at the point of crack initiation, and at the peak load, for comparison. Estimates of the fracture parameters for both dentin specimens are listed in Table 2. The fracture resistance of dentin (energy release rate (G)) calculated for specimens 1 and 2 underwent an increase of 40 and 16 percent, respectively, with crack growth from initiation to the peak load (Table 2).

Typical Moiré fringe patterns on the surface of a dentin specimen undergoing wedge loading are shown in Fig. 8. The fringe patterns in Figs. 8(a) and 8(b) represent the u-displacement field captured during wedge loading at 1.34 and 2.96 mm of crack extension, respectively. Both displacement fields exhibit a sharp fringe deflection away from the crack tip as they near the traction-free surface. A magnified view of the near-tip displacement field in Fig. 8(b) is shown in Fig. 9 and clearly elucidates a region of non-linear behavior, adjacent to the crack tip. The non-linear deformation zone extends approximately 250 μm laterally on each side of the propagating crack; the gradient in displacement with distance from the crack is inconsistent with the displacement field expected from linear elastic theory. Also evident is the appearance of a forked crack tip, which suggests that a microcracking zone has developed in front of the dominant crack tip. Microcracking and bifurcation of the crack were observed in the fringe patterns of both specimens over the range of crack extension.

The Moiré fringe field captured at each increment of crack extension was used to determine the u-field displacement behind the crack according to eq (1), and to calculate the CTOD history during stable crack growth. The relationship between

TABLE 2—ENERGY RELEASE RATE AND FRACTURE TOUGHNESS OF THE DENTIN SAMPLES

Specimen	Crack Initiation		Peak Load	
	G_I (J m^{-2})	K_I (Mpa m$^{0.5}$)	G_I (J m^{-2})	K_I (Mpa m$^{0.5}$)
1	650.6	3.0	943.6	3.6
2	139.6	1.4	164.7	1.5

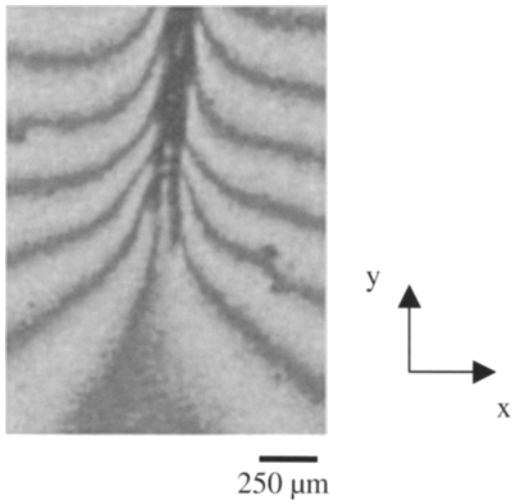

Fig. 9—A magnified view of the Moiré fringe patterns near the crack tip from Fig. 8(a). Note the prevalent non-linearity in the fringe pattern adjacent to the crack boundary

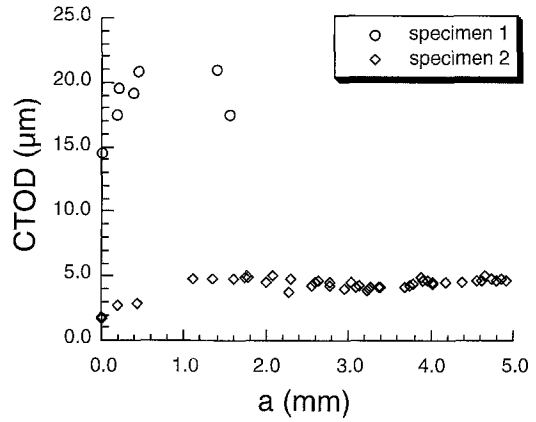

Fig. 10—The CTOD during stable crack growth in the WL-DCB specimens. The CTOD was evaluated 1 mm behind the crack tip

the CTOD and the unit of crack extension in the bovine dentin WL-DCB specimens is shown in Fig. 10. Note that the CTOD profile for specimens 1 and 2 represents a reduction of over 10 and 40 displacement fields, respectively. As expected from the load response profiles (Fig. 10), the CTOD for both dentin specimens initially increased with crack growth. An increase in the CTOD signifies the influence of non-linear deformation contributing to the dissipation in energy. However, the decrease in CTOD that occurs after approximately 1 mm of extension suggests that there may be other mechanisms contributing to the fracture behavior.

Discussion

Flaws are often inadvertently introduced within dentin and enamel during cavity preparation with dental burs. In fact, cracks exceeding 100 μm in length have been found in the sub-surface layers of enamel prepared with abrasive diamond burs.[23] It has also recently been shown that fatigue crack growth of flaws introduced along the cavosurface margin in dentin may play a major role in restoration failure.[24] Therefore, an understanding of the mechanics of fatigue and fracture associated with crack growth in dentin and enamel is highly relevant to tooth fracture and the future of restorative dentistry.

The fatigue crack growth exponent (m) that was estimated for the dentin specimens in this study is consistent with that reported for bone, which reportedly ranges from 2.8 to 5.1.[25] However, the rate of fatigue crack growth in the DCB dentin specimens did not agree well with results obtained from cyclic loading of the WL-DCB specimens, as evident from Table 1.[26] Friction between the dentin and stainless-steel pin, and microcracking damage observed beneath the pin contact complicated the use of the wedge-load configuration. These factors dissipated the energy available for crack propagation and suppressed the fatigue crack growth at low stress intensities. Based on a comparison of results and the fractured surface from specimens with both configurations, the standard DCB specimen provides a more reliable geometry for the study of fatigue crack growth in bovine dentin.

The rate of cyclic crack growth in dentin has not been previously reported. Results from this preliminary study suggest that the rate of fatigue crack growth in dentin is larger for crack propagation perpendicular to the dentin tubules. The results agree with observations from restored teeth in which cracks are typically oriented perpendicular to the dentin tubules. Furthermore, although a longitudinal groove was introduced to guide crack growth, crack curving occurred frequently, especially in the specimens with dentin tubules oriented parallel to the direction of crack growth. Near-tip microcracking and unstable growth were also observed and complicated the fatigue crack growth experiments. These difficulties limit the cyclic crack growth measurements and may be attributed to preferential growth perpendicular to the dentin tubules. Additional experiments are necessary for confirmation of the observations and to provide further understanding of the mechanisms of fatigue crack growth in dentin.

The energy release rate (G) and fracture toughness (K) of the bovine dentin samples were estimated assuming isotropy and ideal brittle material response according to Griffith's model. Note that this approach is an approximation for a true DCB specimen, which is restricted to opening loads and neglects the contribution of friction between the steel pin and specimen surface resulting from wedge loading. Nevertheless, results obtained in this study are in agreement with values of G and K reported for bovine and human dentin in

the literature.[10–12,27,28] As evident from the Moiré fringe patterns in Figs. 8 and 9, there is a component of non-linear deformation surrounding the crack tip in dentin that contributes to the energy dissipated during fracture. It is generally accepted that the load crack extension plot of an ideally brittle material should be flat whereas a rising curve signifies either local crack tip non-linearity associated with non-elastic deformation (i.e., plastic deformation or microcracking) and/or development of a fracture process zone (FPZ).[22,29] Consequently, Griffith's criterion and the use of Irwin's model are not appropriate for evaluating the fracture behavior of dentin, and the quantities in Table 2 should be considered approximations only. The dissipation of fracture energy through extensive plastic deformation has also been documented within the DEJ of bovine chevron notched samples by Lin and Douglas.[11] Dentin has been previously described in the literature as isotropic and brittle in which the fracture process was described assuming linear elastic response. These assertions were based on observations of the fractured surfaces without detailed knowledge of the displacement field surrounding the crack tip and clear evidence of non-linear deformation. But based on the Moiré fringe fields, the fracture of mineralized dentin appears to be an elastic-plastic process and is influenced by the presence of a FPZ. Although the relative contribution of near-tip non-linear deformation to energy dissipation remains unknown, it may play an important role in tooth fracture resistance of dentin. Note that isotropic behavior was assumed in evaluating the stress intensity at fracture in the WL-DCB specimens. Models are available for analyzing the stress intensity in anisotropic materials[30] and may be utilized in the future as further understanding of crack growth in dentin is developed. Unfortunately, tubule orientations of the WL-DCB specimens were not documented after completion of the experiments. This presents a critical limitation to understanding differences in crack growth and fracture in the two dentin specimens.

It is reasonable to believe that the physical construction of dentin promotes damage tolerance and would serve to arrest flaws initiated within the more brittle enamel. In fact, cracks in the enamel of teeth *in vivo* always stop at the DEJ. Damage tolerant materials generally exhibit a rising toughness with crack extension.[29] Indeed, the load crack extension curves in Fig. 7 and the CTOD profiles in Fig. 10 suggest that dentin exhibits toughening behavior. Through the development of a FPZ in front of the crack tip, energy is dissipated within microstructural elements with crack extension. The contribution of a secondary FPZ behind the crack tip could not be seen through the wedge load response or Moiré fringe fields. However, the post-plateau decrease in CTOD, which is observed from both specimens in Fig. 10, implies that a secondary FPZ developed in the dentin that invoked a closure stress. An earlier examination of fractured dentin[31] has suggested that collagen fibers provide reinforcement to the brittle mineralized matrix; fractured surfaces have exhibited evidence of collagen fibers bridging the crack face. Rasmussen *et al.*[27] found that the fracture of dentin was anisotropic and that the material's toughness was greatest for fracture parallel to the dentin tubules due to the collagen network. These bridging networks may foster development of a posterior crack closure stress, which contributes to the dissipation of fracture energy. Observation of the fracture surfaces of the DCB dentin fatigue specimens revealed pertibular cuffs pulled out from the intertubular matrix. Either of these mechanisms could have contributed to the rising load crack extension response observed in Fig. 7 through the development of crack closure stresses.

The inter-relationship between collagen fibers and the dentinal matrix undergoes changes with demineralization[32] and aging.[33] Thus, the contribution of a frontal and/or posterior FPZ to energy dissipation during the fracture of dentin may not remain constant over the life of a tooth. The demineralization of dentin has been found to result in significant reductions of the ultimate tensile strength and elastic modulus.[16] Hence, it is reasonable to believe that the FPZ contributions to fatigue and fracture resistance would be diminished with demineralization as well. To evaluate this assertion, it would be necessary to dissect the individual contributions of the frontal and posterior FPZ to the total energy dissipated during crack growth. Our future work will focus on the mechanisms of energy dissipation in the fatigue and fracture of dentin and their importance to the success of restorative dentistry.

Conclusions

An experimental *in vitro* analysis of the mechanics of fatigue and fracture in bovine dentin has been conducted. Based on the results from this preliminary study, the following conclusions are drawn:

1. The rate of fatigue crack growth in bovine dentin is dependent on the tubule orientation. Preliminary results suggest that the rate of crack growth is largest for crack propagation oriented perpendicular to the dentin tubules.

2. The wedge-load response and crack tip opening displacement with crack extension increased with crack extension. These observations indicate that bovine dentin exhibits an increasing fracture toughness with crack extension (rising R-curve behavior).

3. Displacement fields documented during stable crack growth using Moiré interferometry suggest that a FPZ contributed to the fracture of dentin. Furthermore, the fracture of dentin is comprised of linear elastic and nonlinear deformation and is evident from fringe deflection near the crack tip.

Acknowledgments

This work was partially supported through a biomedical engineering research grant from the Whitaker Foundation and an equipment grant from the National Science Foundation (BES-9900196). The authors are grateful to Prof. Albert Kobayashi and Dr Duc Tran for their help with preliminary experiments conducted at the University of Washington and to Dr Bhavna Shroff and Dr Murray Sarubin for their suggestions and comments. Many helpful comments were also received from Prof. Grayson Marshall and Prof. Dave Pashley in interpreting the results and with regards to the structural and mechanical properties of dentin.

References

1. Letzel, H., van't Hof, M.A., Vrijhoef, M.M.A., Marshall, G.W. Jr, and Marshall, S.J., "A Controlled Clinical Study of Amalgam Restorations: Survival, Failures, and Causes of Failure," Dent. Mater., **5**, *115–121 (1989).*

2. Gher, M.E. Jr, Dunlap, R.M., Anderson, M.H., and Kuhl, L.V., "Clinical Survey of Fractured Teeth," J. Am. Dent. Assoc., **114**, 174–177 (1987).

3. Eakle, W.S., Maxwell, E.H., and Braly, B.V., "Fractures of Posterior Teeth in Adults," J. Am. Dent. Assoc., **112**, 215–218 (1986).

4. Cameron, C.E., "The Cracked Tooth Syndrome: Additional Findings," J. Am. Dent. Assoc., **93**, 971–975 (1976).

5. Ten Cate, A.R., "Oral Histology. Development Structure and Function," Mosby (1980).

6. Marshall, G.W. Jr, Marshall, S.J., Kinney, J.H., and Balooch, M., "The Dentin Substrate: Structure and Properties Related to Bonding," J. Dent., **25**, 441–458 (1997).

7. Kinney, J.H., Balooch, M., Marshall, S.J., Marshall, G.W. Jr, and Weihs, T.P., "Atomic Force Microscope Measurements of the Hardness and Elasticity of Peritubular and Intertubular Dentin," J. Biomech. Eng., **118**, 133–135 (1996).

8. Kinney, J.H., Balooch, M., Marshall, G.W. Jr, and Marshall, S.J., "Elastic Properties of Dentin are not Affected by Tubule Orientation," J. Dent. Res., **78**, 3468 (1999).

9. Kinney, J.H., Marshall, S.J., and Marshall, G.W. Jr, "The Mechanical Properties of Human Dentin: A Critical Review and Reevaluation of the Dental Literature," Crit. Rev. Oral Biol. Med. (in press)

10. Xu, H.H.K., Smith, D.T., Jahanmir, S., Romberg, E., Kelly, J.R., Thompson, V.P., and Rekow, E.D., "Indentation Damage and Mechanical Properties of Human Enamel and Dentin," J. Dent. Res., **77**, 472–480 (1998).

11. Lin, C.P., and Douglas, W.H., "Structure-property Relations and Crack Resistance at the Bovine Dental-Enamel Junction," J. Dent. Res., **73**, 172–178 (1994).

12. el Mowafy, O.M., and Watts, D.C., "Fracture Toughness of Human Dentin," J. Dent. Res., **65**, 677–681 (1986).

13. Hassan, R., Caputo, A.A., and Bunshah, R.F., "Fracture Toughness of Human Enamel," J. Dent. Res., **60**, 820–827 (1981).

14. Okazaki, K., Nishimura, F., and Nomoto, S., "Fracture Toughness of Human Enamel," Shika Zairyo Kikai, **8**, 382–387 (1989).

15. Iwamoto, N., and Ruse, N.D., "NTP Specimen Fracture Toughness Test Applied to Human Dentin," Proc. SEM Annual Conf. and Exposition on Experimental and Applied Mechanics, Portland OR, 90-91 (2001).

16. Sano, H., Ciucchi, B., Matthews, W.G., and Pashley, D.H., "Tensile Properties of Mineralized and Demineralized Human and Bovine Dentin," J. Dent. Res., **73**, 1205–1211 (1994).

17. Jameson, M.W., Hood, J.A., and Tidmarsh, B.G., "The Effects of Dehydration and Rehydration on Some Mechanical Properties of Human Dentine," J. Biomech., **26**, 1055–1065 (1993).

18. Schilke, R., Lisson, J.A., BauB, O., and Geurtsen, W., "Comparison of the Number and Diameter of Dentinal Tubules in Human and Bovine Dentine by Scanning Electron Microscope Investigation," Arch. Oral Biol., **45**, 355–361 (2000).

19. Schilke, R., BauB, O., Lisson, J.A., Schuckar, M., and Geurtsen, W., "Bovine Dentin as a Substitute for Human Dentin in Shear Bond Strength Measurements," Am. J. Dent., **12**, 92–96 (1999).

20. Paris, P.C., and Erdogan, F., "A Critical Analysis of Crack Propagation Laws," J. Basic Eng., **D 85**, 528–534 (1963).

21. Post, D., "Moiré Interferometry," in Handbook on Experimental Mechanics, 297–364, 2nd ed., ed. A.S. Kobayashi, VCH, New York (1993).

22. Anderson, T.L., "Fracture Mechanics: Fundamentals and Applications," 1st ed., 50–62, Boca Raton, FL: CRC Press (1991).

23. Xu, H.H.K., Kelly, J.R., Jahanmir, S., Thompson, V.P., and Rekow, E.D., "Enamel Subsurface Damage due to Tooth Preparation with Diamonds," J. Dent. Res., **76**, 1698–1706 (1997).

24. Arola, D., Huang, M.P., and Sultan, M.B., "The Failure of Amalgam Restorations due to Cyclic Fatigue Crack Growth," J. Mater. Sci.: Mater. Med., **10**, 319–327 (1999).

25. Wright, T.M., and Hayes, W.C., "The Fracture Mechanics of Fatigue Crack Propagation in Compact Bone," J. Biomed. Mater. Res., **10**, 637–648 (1976).

26. Arola, D., and Rouland, J., "An Experimental Evaluation of Cyclic Crack Growth in Mature Bovine Dentin," Proc. SEM Annual Conference on Theoretical, Experimental and Computational Mechanics. Portland, OR, June 4-6, 780–782 (2001).

27. Rasmussen, S.T., Patchin, R.E., Scott, D.B., and Heuer, A.H., "Fracture Properties of Human Enamel and Dentin," J. Dent. Res., **55**, 154–164 (1976).

28. Rasmussen, S.T., and Patchin, R.E., "Fracture Properties of Human Enamel and Dentin in an Aqueous Environment," J. Dent. Res., **63**, 1363–1368 (1984).

29. Lawn, B., "Fracture of Brittle Solids," 2nd ed., Cambridge University Press (1993).

30. Sih, G.C., Paris, P.C., and Irwin, G.R., "On Cracks in Rectilinearly Anisotropic Bodies," Int. J. Fract. Mech., **1**, 189–203 (1965).

31. Spector, M., and Taylor, S.E., "Fracture of Human Dentin: A High Resolution Scanning Electron Microscope Study," J. Dent. Res., **55**, 1136 (1976).

32. Van Meerbeek, B., Dhem, A., Goret-Nicaise, M., Braem, M., Lambrechts, P., and Vanherle, G., "Comparative SEM and TEM Examination of the Ultrastructure of the Resin-Dentin Interdiffusion Zone," J. Dent. Res., **72**, 495–501 (1993).

33. Prati, C., Chersoni, S., Mongiorgi, R., Montanari, G., and Pashley, D.H., "Thickness and Morphology of Resin-infiltrated Dentin Layer in Young, Old, and Sclerotic Dentin," Oper. Dent., **24**, 66–72 (1999).